NO Reductase from *Bacillus azotoformans* Is a Bifunctional Enzyme Accepting Electrons from Menaquinol and a Specific Endogenous Membrane-Bound Cytochrome c_{551}†

Suharti, Hendrik A. Heering, and Simon de Vries*

Department of Biotechnology, Delft University of Technology, Julianalaan 67, 2628 BC Delft, The Netherlands

Received June 8, 2004; Revised Manuscript Received July 25, 2004

ABSTRACT: *Bacillus azotoformans* is a Gram-positive denitrifying soil bacterium, which is capable of respiring nitrate, nitrite, nitric oxide, and nitrous oxide under anaerobic conditions. It contains a unique menaquinol-dependent nitric oxide reductase (qCu$_A$NOR) with a Cu$_A$ center in its small subunit. The qCu$_A$NOR exhibits menaquinol-dependent NO reductase activity, whereas reduced horse heart cytochrome *c* was inactive. Here we describe the purification of three membrane-bound *c* cytochromes from *B. azotoformans*. Their apparent molecular masses on SDS−PAGE are approximately 11 kDa. At neutral pH, these *c* cytochromes are negatively charged and the E_m for all is close to 150 mV. Only one of these *c* cytochromes, which exhibits an α-band maximum at 551 nm, acts as a direct electron donor to qCu$_A$-NOR. Further investigation demonstrated that this cytochrome c_{551} possesses two lipoyl moieties, which presumably function to anchor it to the membrane. Steady-state kinetic studies reveal that cytochrome c_{551} is a noncompetitive inhibitor of NO reduction when menaquinol is used as an electron donor. This finding points to the presence of two different electron donation pathways in qCu$_A$NOR. The ability of qCu$_A$NOR to accept electrons from both menaquinol and cytochrome c_{551} might be related to the regulation of the rate of NO reduction especially as a defense mechanism of *B. azotoformans* against the toxicity of NO. Growth experiments in batch culture indeed show that *B. azotoformans* is highly NO tolerant, in contrast to, for example, *Paracoccus denitrificans* that has a monofunctional cytochrome *c*-dependent NOR. We propose that the menaquinol pathway, which has a 4-fold greater maximal activity than the pathway via cytochrome c_{551}, is used for NO detoxification, whereas electron donation via the endogenous cytochrome *c* involves the cytochrome b_6f complex serving the bioenergetic needs of the organism.

Denitrification is one of the main branches in the global nitrogen cycle, which yields nitrogen gas from nitrate via nitrite, nitric oxide, and nitrous oxide (*1*). A key enzyme in denitrification is nitric oxide reductase (NOR),[1] which is responsible for the formation of the N−N bond. Three types of bacterial NORs have been purified so far (*2*, *3*), and they all belong to the superfamily of heme-copper oxidases. The first type is a cytochrome *bc* complex, cNOR. This type of NOR has been purified from Gram-negative bacteria, e.g., *Paracoccus denitrificans*, *Pseudomonas stutzeri*, and *Paracoccus halodenitrificans* (*4*−*7*). The purified cNORs consist of two subunits: a heme *c*-containing subunit (NorC) and a heme *b*-containing subunit (NorB). The physiological electron donors of cNOR are membrane-bound and soluble cytochrome *c* or pseudoazurin (*1*, *8*−*11*). The primary electron acceptor in cNOR is the heme *c* in the NorC subunit. Subsequently, the electron is transferred to a low-spin heme *b* and finally to a dinuclear center where the reduction of NO occurs.

The second type of NOR is a menaquinol-dependent NOR (qNOR) as purified from *Ralstonia eutropha* (*12*) or the hyperthermophilic archaeon, *Pyrobaculum aerophilum* (*13*). The purified qNOR consists of a single subunit and compared to NorB contains an N-terminal extension of ∼280 amino acid residues proposed to bind quinone. Sequence analysis indicates that this extension can fold into two transmembrane α-helices connected by a hydrophilic domain (*14*). Surprisingly, the sequence of this N-terminal extension is similar to that of the NorC subunit of cNORs. Therefore, qNOR has been suggested to be a fusion of NorC and NorB that has lost the heme *c* center and obtained a quinol-binding site during evolution (*14*).

The third type of NOR is a two-subunit NOR, qCu$_A$NOR, which has been purified so far only from the Gram-positive bacterium *Bacillus azotoformans* (*15*). The purified qCu$_A$-NOR exhibits a menaquinol-dependent NO reductase activity and contains Cu$_A$ in the small subunit, which is unique to NORs. The Cu$_A$ center is known as an electron carrier in cytochrome *c* oxidases (e.g., cytochrome aa_3 oxidase, cytochrome caa_3 oxidase, and cytochrome ba_3 oxidase) and nitrous oxide reductase; in all these enzymes, Cu$_A$ accepts electrons from cytochrome *c* (*16*−*20*). In qCu$_A$NOR, ascor-

† This study has been financed by a grant from the Indonesian Ministry of Education to Suharti and by the European Union program Biotechnology (Project SENORA BIO4-98-0507).

* To whom correspondence should be addressed. Fax: +31 15 2782355. E-mail: s.devries@tnw.tudelft.nl.

[1] Abbreviations: NOR, NO reductase; NIR, nitrite reductase; NAR, nitrate reductase; qCu$_A$NOR, menaquinol- and cytochrome c_{551}-dependent nitric oxide reductase; PMS, phenazine methosulfate.

10.1021/bi0488101 CCC: $27.50
Published on Web 10/02/2004

bate can act as a substrate directly. However, reduced horse heart cytochrome *c* was inactive with qCu_ANOR, although it did stimulate the activity in the presence of ascorbate and PMS. Since many Cu_A-containing oxidases can be assayed with horse heart cytochrome *c*, it seemed likely that qCu_A-NOR would contain a cytochrome *c* binding site, too, in addition to that for menaquinol. The cytochrome *c* binding site is thus expected to be analogous to that in Cu_A-containing cytochrome *c* oxidases, and we considered the possibility that only a specific endogenous cytochrome *c* of *B. azotoformans* would be able to donate electrons efficiently to this site.

In this communication, we report the purification of membrane-bound *c*-type cytochromes from *B. azotoformans* and their interaction with qCu_ANOR. We have purified three different cytochrome *c* species from *B. azotoformans* membranes; one of these was found to be capable of donating electrons to qCu_ANOR. Since menaquinol is capable of donating electrons to qCu_ANOR as well, this makes qCu_A-NOR a unique bisubstrate NO reductase. We propose that the menaquinol- and cytochrome *c*-dependent pathways are active in NO detoxification and in denitrification, respectively.

EXPERIMENTAL PROCEDURES

Purification of Endogenous Membrane-Bound Cytochrome c. B. azotoformans was grown anaerobically, and membranes were purified as described in ref *15*. The membranes from 200 g of wet weight cells were diluted to 10 mg/mL protein in 50 mM Bis-Tris buffer (pH 6.5) containing 1 mM EDTA. Dodecyl maltoside was added dropwise to a final concentration of 0.6% (w/v) from a 10% stock solution, with slow stirring. The suspension was then incubated on ice for 15 min and centrifuged at 150000*g* for 60 min. The clear supernatant was applied directly to a Q-Sepharose column (5 cm × 20 cm) equilibrated with 20 mM Bis-Tris (pH 6.5), 1 mM EDTA, and 0.03% dodecyl maltoside. The column was washed with 1 bed column volume of the equilibration buffer, and elution was performed with a linear NaCl gradient (from 0 to 0.5 M). Fractions containing cytochrome *c* stimulating NOR activity eluted between 0.1 and 0.2 M NaCl and actually coeluted with NOR. The cytochrome *c* was then separated from NOR by passing it through a Bio-Scale Ceramic hydroxyapatite column equilibrated with 10 mM potassium phosphate buffer (pH 7) containing 0.1% dodecyl maltoside. Cytochrome *c* did not bind while NOR was retained by the column. Cytochrome *c* fractions were then applied to a butyl-Sepharose column equilibrated with 20 mM phosphate buffer (pH 7), 1 M ammonium sulfate, and 0.2% dodecyl maltoside. Before the samples were applied to the butyl-Sepharose column, solid ammonium sulfate was added to a final concentration of 1 M and the mixture incubated on ice for 1 h. Elution was performed by a decreasing linear ammonium sulfate gradient (from 1.0 to 0.0 M), and the cytochrome *c* fraction eluted between 0.3 and 0.1 M ammonium sulfate. Fractions were pooled, and ammonium sulfate was removed by dialysis using a dialysis membrane with a 3.5 kDa cutoff. The ammonium sulfate free fraction was then applied to a Mono Q column (1 cm × 10 cm) equilibrated with 20 mM Tris-HCl (pH 8) and 0.1% dodecyl maltoside. After the column had been washed with 1 bed volume, elution was performed with a NaCl gradient (from 0 to 0.5 M), and the cytochrome *c* fraction eluted between 0.3 and 0.4 M NaCl. Final separation was performed using an isoelectric focusing column (Mono P). The Mono P column was equilibrated first with Bis-Tris-HCl (pH 6.3) containing 0.05% lauryl maltoside. The cytochrome *c* fraction was equilibrated with the same buffer. Elution was performed with polybuffer PBE 7-4 (Amersham Bioscience). In this pH range, two fractions of cytochrome eluted at pH ~5 ± 0.5 and ~4 ± 0.5, and a red band remained bound to the column. This latter red fraction eluted with water and had an apparent pI of 3 ± 0.5 on the isoelectric column.

Cyclic Voltammetry. For voltammetry, a 10 μL droplet containing 50−150 μM protein [in 20 mM potassium phosphate buffer (pH 7.0) with 1 mM EDTA and 0.03% dodecyl maltoside] was placed between the tip of the reference electrode and the horizontal working electrode disk (wetted electrode area ± 10 mm^2). The working electrode was a 12 mm diameter glassy carbon disk (type V25, Le Carbon Loraine), polished with 6 μm Metadi Diamond Compound spray on a Microcloth polishing cloth (both from Buehler), rinsed with water, and dried. The polished glassy carbon is rich in oxidized carbon functionalities, and therefore will not be sufficiently hydrophobic to promote the adsorption of a blocking monolayer of surfactant, especially not at the low concentration of dodecyl maltoside present in the solution (0.03%).

The reference was a saturated calomel electrode (SCE) with porous pin (Radiometer K401), and a platinum wire was used as the counter electrode. The electrodes and droplet of solution were mounted in a closed glass setup (*21*), which was flushed with wetted argon. Staircase cyclic voltammetry was performed with an Autolab PSTAT 10 electrochemical analyzer (EcoChemie) equipped with an Electrochemical Detection module for increased sensitivity, and controlled by GPES 4.8 software. All potentials are reported with reference to the normal hydrogen electrode (NHE), based on a potential of 244 mV for the SCE at 25 °C.

Small-Scale Growth of Cells for Studying NO Tolerance. B. azotoformans and *Pa. denitrificans* were grown aerobically and anaerobically as described in refs *15* and *7*, respectively. A 100 mL bottle was filled with 20 mL of cell suspension from aerobically (OD_{600} = 0.6) or anaerobically (OD_{600} = 0.6) grown cultures of *B. azotoformans* or *Pa. denitrificans.* The cell suspensions were then incubated for 2 h under 5% NO (yielding a 100 μM NO solution) under continuous stirring. After this treatment, the cells were serially diluted, plated on brain heart infusion agar, and grown aerobically for 20 h at 34 °C. The number of colonies was compared to the number in similarly treated control cells, incubated without NO.

Miscellaneous. The qCu_ANOR was purified according to the method described in ref *15*, and NO reductase activity was measured according to methods described in refs *7* and *15*. To determine the nature of the covalently bound lipid, purified cytochrome *c* was incubated with lipase from *Rhizopus arrbizus* (Sigma). The digested cytochrome *c* was then applied to a 1 mL butyl-Sepharose column. The column was equilibrated with water containing 0.1% TFA, and cytochrome *c* was eluted with a linear acetonitrile gradient containing 0.1% TFA. Both native PAGE and SDS−PAGE were performed using the Phastgel Homogenous High-

Table 1: Properties of Cytochrome *c* Fractions Eluted from a MonoP Column

	pI[a]	absorbance maxima γ-, β-, and α-bands (nm)	midpoint potential (mV)	molecular mass (kDa)	NOR activity stimulation
cytochrome c_{551}	5 ± 0.5	415.2, 522.2, 550.9	143	10.8 ± 0.2	yes
cytochrome c_{550}	4 ± 0.5	415.8, 521.9, 550.5	147	10.8 ± 0.2	no
cytochrome c_{552}	3 ± 0.5	416.2, 522.9, 551.6	154	10.8 ± 0.2	no

[a] The pI was determined using isoelectric focusing PAGE and MonoP column chromatography.

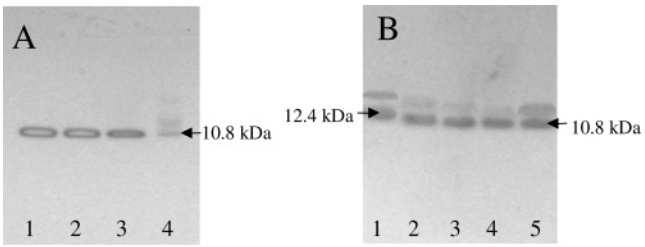

FIGURE 1: Native PAGE and SDS−PAGE of purified *c* cytochromes. (A) Native PAGE of membrane-bound cytochromes purified from the cytoplasmic membrane of *B. azotoformans*. Lanes 1−3 contained cytochrome c_{552}, cytochrome c_{550}, and cytochrome c_{551}, respectively; lane 4 contained cytochrome c_{551} purified from *Ps. aeruginosa*. (B) SDS−PAGE pattern of membrane-bound cytochromes purified from the cytoplasmic membrane of *B. azotoformans*. Lanes 1−5 contained horse heart cytochrome *c*, cytochrome c_{552}, cytochrome c_{550}, cytochrome c_{551}, and cytochrome c_{551} from *Ps. aeruginosa*, respectively.

Density system purchased from Pharmacia. Denatured cytochrome *c* was prepared in the presence of 6 M urea. Heme staining was performed using the method described by Thomas *et al*. (*22*). UV−vis spectra were recorded using a DW2000 UV−vis spectrophotometer. Nitrate reductase and nitrite reductase activities were measured using reduced plumbagin as the electron donor, and NADH dehydrogenase was measured using plumbagin as the electron acceptor. Reduction or oxidation of plumbagin was monitored spectroscopically at 419 nm ($\epsilon = 3.95$ mM^{-1} cm^{-1}). Cytochrome b_6f activity was measured using reduced plumbagin as the electron donor, and the reduction of horse heart cytochrome *c* was monitored spectroscopically at 550 nm ($\epsilon = 20.5$ mM^{-1} cm^{-1}).

RESULTS

Purification and Characterization of Membrane-Bound c Cytochromes. Three types of membrane-bound *c* cytochromes (cytochrome c_{550}, c_{551}, and c_{552}) were successfully purified from the cytoplasmic membranes of *B. azotoformans*. Six steps of column chromatography which included ion exchange, ceramic hydroxyapatite, hydrophobic interaction chromatography, and finally isoelectric focusing column chromatography (Mono P) were employed. Three cytochromes apparently copurified in the first five columns and were separated only on the isoelectric focusing column. Table 1 summarizes the features of the three cytochromes. They are negatively charged at neutral pH with apparent isoelectric focusing points of 5.0 ± 0.5, 4.0 ± 0.5, and 3.0 ± 0.5 for cytochrome c_{551}, cytochrome c_{550}, and cytochrome c_{552}, respectively. Under native and denaturing conditions, all three cytochromes migrated with apparent molecular masses of approximately 11.0 kDa (Figure 1). On SDS−PAGE in the presence of 6 M urea, the three cytochromes from *B. azotoformans* and both horse heart cytochrome *c* and cytochrome c_{551} from *Pseudomonas aeruginosa* displayed two bands. The faint upper bands correspond most likely to partially denatured forms. Figure 2 shows UV−vis spectra of the oxidized and reduced state of each type of cytochrome *c*. The α-bands had slightly but clearly different maxima; the three cytochromes are named after their α-band maxima (see also Table 1). EPR spectroscopy indicated that all three cytochromes display highly anisotropic spectra with a g_z of 3.45, characteristic of low-spin hemes (data not shown).

NOR activity assays using the endogenous membrane-bound *c* cytochromes (at 140 μM) revealed a stimulating activity only in the presence of reduced cytochrome c_{551} (Figure 3A). After addition of qCu_ANOR to the buffer containing NO and reduced cytochrome c_{551}, a significant rate of NO consumption was achieved. The slope of the activity traces employing the two other cytochromes did not change after addition of qCu_ANOR (data not shown), indicating less than 1% of the stimulating activity obtained with cytochrome c_{551}. The calculated maximum turnover number with cytochrome c_{551} as the electron donor is 41 NO/s. This is lower than the maximal turnover number obtained with menaquinol, which was 153 NO/s (*15*). A Lineweaver−Burk plot yields an apparent K_m of 4.5 μM for cytochrome c_{551} (Figure 3B).

Small *c* cytochromes are anchored to the membrane via a transmembrane α-helix or by (close to) N-terminal covalently bound lipids (*23*−*26*). Cytochrome c_{511} is anchored to the membrane via a covalently bound lipid. Figure 4 displays the elution profile on the butyl-Sepharose column of undigested and partially lipase digested cytochrome c_{551}. Undigested cytochrome c_{551} migrates as a single peak. Two additional peaks with shorter elution times were obtained after incubation with lipase for 3 and 7 h. These two peaks likely represent cytochrome c_{511} having lost one and two lipoyl moieties, respectively (*23*, *27*). Unfortunately, because of proteolytic activity in the lipase preparation, incubation could not be performed for periods longer than 7 h, preventing complete conversion (data not shown).

The electrochemical properties of the three cytochromes were studied with cyclic voltammetry. As shown in Figure 5, stable quasi-reversible voltammograms were obtained for all three fractions. Midpoint potentials of 143, 147, and 154 mV versus the NHE are determined for cytochrome c_{550}, cytochrome c_{551}, and cytochrome c_{552}, respectively, and are independent of scan rate. The peak amplitudes increase proportionally with the square root of the scan rate, as expected for diffusion of the cytochromes to the electrode surface (data not shown). However, the peak separations are larger than the expected separation of 58 mV for diffusion-limited voltammetry. Even at a scan rate as low as 2 mV/s, the peak separations are still 79, 96, and 83 mV for cytochrome c_{550}, cytochrome c_{551}, and cytochrome c_{552}, respectively. At higher scan rates, the voltammograms

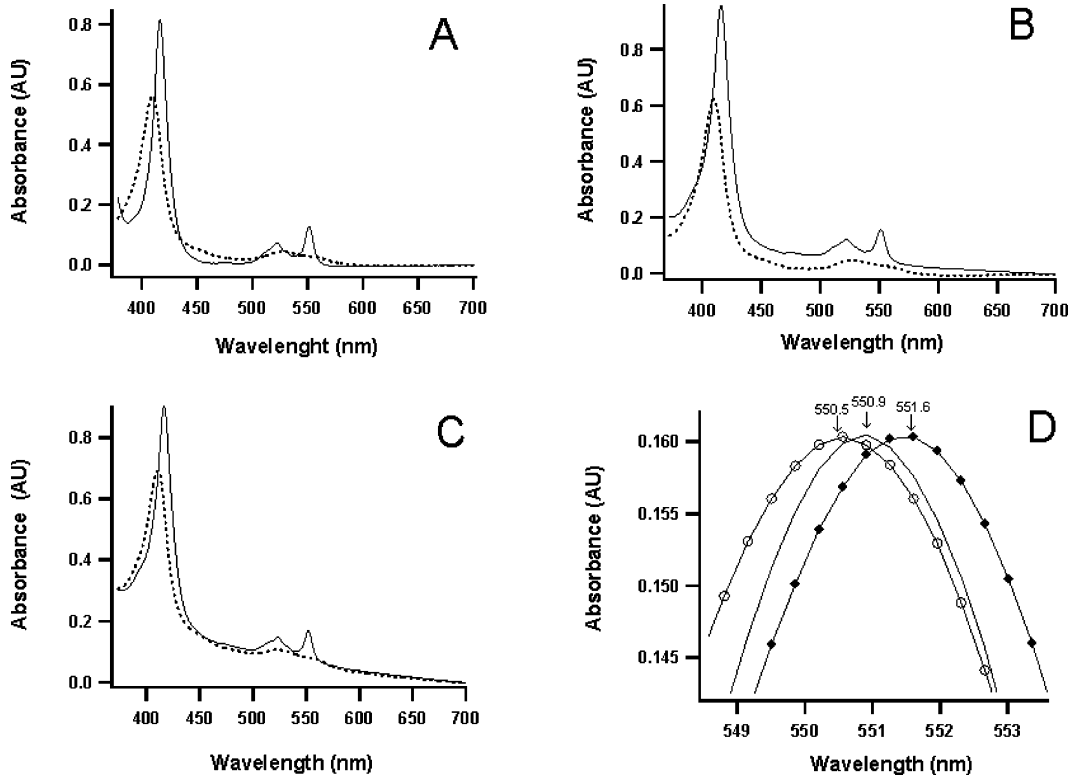

FIGURE 2: UV−vis spectra of membrane-bound cytochromes. (A−D) Oxidized state (···) and dithionite-reduced state (- - -): (A) cytochrome c_{550}, (B) cytochrome c_{551}, and (C) cytochrome c_{552}. (D) Overlay of spectra of dithionite-reduced samples of the α-band region of cytochrome c_{550} (○), cytochrome c_{551} (—), and cytochrome c_{552} (◆).

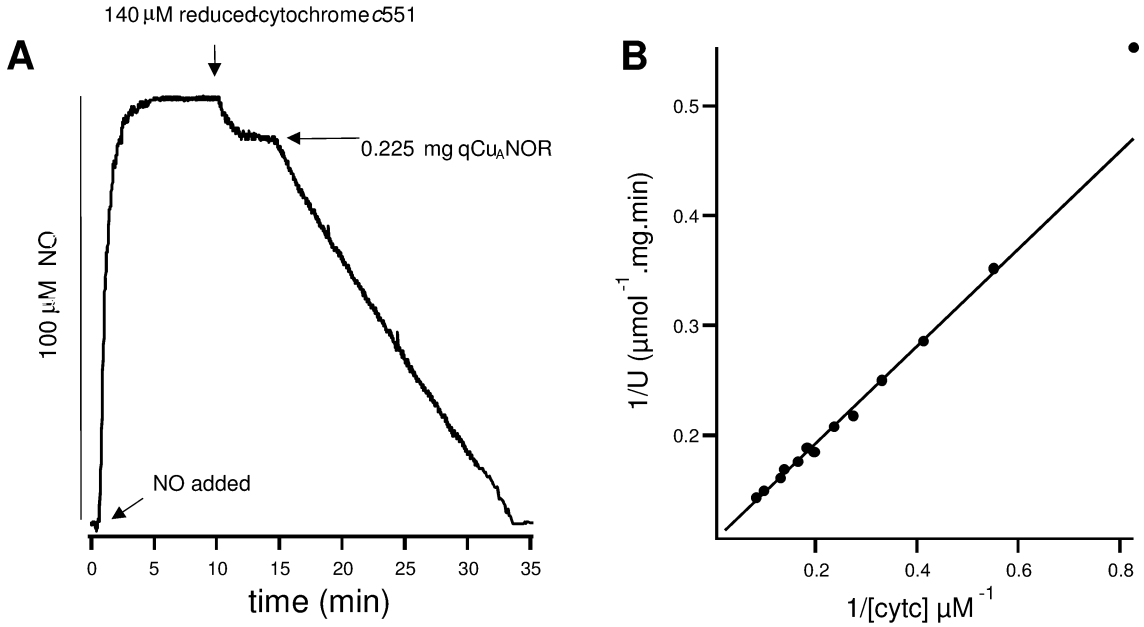

FIGURE 3: Stimulation of the qCu_ANOR activity by cytochrome c_{551}. (A) After anaerobiosis ($t = 0$), 5% NO gas was flushed into the reaction vial, yielding a solution of 100 μM NO. Reduced cytochrome c_{551} and qCu_ANOR were then added (note that traces of oxygen in the solution of cytochrome c_{551} lead to a rapid, albeit small, decrease in the NO concentration directly after the addition of 140 μM cytochrome c_{551}). (B) Lineweaver−Burk plot of $1/qCu_ANOR$ activity vs 1/[cytochrome c_{551}]. In these experiments, the reduced cytochrome was regenerated by ascorbic acid.

broaden further, yielding increasing peak separations, but constant midpoint potentials.

Steady-State Kinetics with Menaquinol Derivatives and Endogenous Cytochrome c_{551}. Since the menaquinol menadiol is relatively poorly soluble in aqueous solution, we have studied alternative substrates as electron donors. Three different hydroxylated naphthoquinols were studied for this purpose, plumbagin (5-hydroxy-2-methyl-1,4-naphthoquinol), juglone (5-hydroxy-1,4-naphthoquinol), and lapachol [2-hydroxy-3-(3-methyl-2-butenyl)-1,4-naphthoquinol] with $E_{m,7}$ values of −40, −33, and −310 mV, respectively. The midpoint potential of menaquinol is −74 mV (*28*). Plumbagin and juglone were active with qCu_ANOR, in contrast to lapachol. Figure 6A displays a curved NO reductase

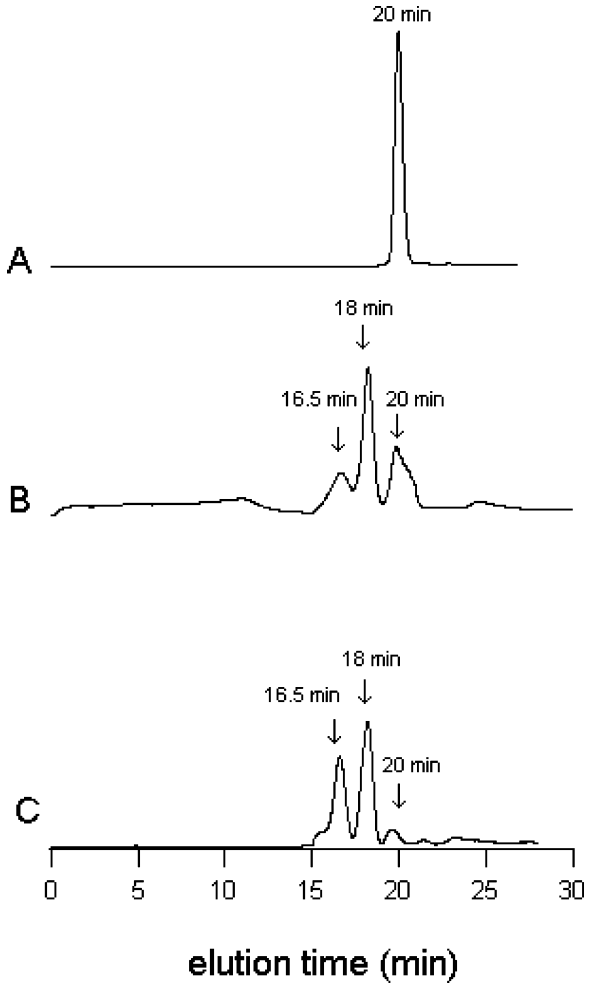

FIGURE 4: Elution profile of cytochrome c_{551} treated for various times with lipase. (A) Undigested cytochrome c_{551} eluting after 20 min. Spectra B and C are cytochrome c_{551} after digestion with lipase for 3 and 7 h, respectively, yielding two additional peaks with shorter elution time at 18 and 16.5 min, respectively.

activity trace with plumbagin (or juglone, not shown) as the electron donor. Nonlinear activity traces have been observed before by employing ascorbate and PMS as the electron donor (*7*) or menaquinol (*13*). The nonlinear traces are due to NO substrate inhibition caused by the formation of a ferric−nitrosyl intermediate (*13*). The K_m values for plumbagin and juglone are determined to be 256 and 141 μM (Figure 6B), respectively. The maximum turnover numbers with plumbagin and juglone as the electron donor are 150 and 118 NO/s, respectively. We have chosen plumbagin for further study for two reasons. First, the turnover number is higher than that of juglone. Second, the structure of plumbagin is more similar to that of the natural menaquinol regarding the presence of a methyl group at position 2 of the naphthalene ring.

A steady-state kinetic study using both plumbagin and cytochrome c_{551} as electron donors was performed. Figure 7A shows the effect of oxidized cytochrome c_{551} on the plumbagin-dependent activity. After addition of the enzyme, a slow NO consumption was observed due to the presence of the electron donor ascorbic acid. After addition of reduced plumbagin (260 μM), the rate of NO consumption increased to a similar rate as seen in Figure 6A. When ~20% of the total NO concentration (25 μM) was consumed, oxidized cytochrome c_{551} was added to a final concentration of 75 μM. An increase in the rate of NO consumption was still observed, similar to the NO consumption when plumbagin is used as the electron donor (see Figure 6A) because of the decrease in the extent of NO substrate inhibition. After approximately half of the total NO concentration was consumed, the cytochrome c_{551} became reduced by ascorbate and the rate of NO consumption decreased. In other words, the electron flow via cytochrome c_{551} to qCu$_A$NOR inhibits the electron flow from reduced plumbagin. Figure 7B shows a noncompetitive pattern of inhibition for electron delivery by plumbagin and ferrocytochrome c_{551}, suggesting the presence of the different binding sites for the two substrates menaquinol, a natural quinol in *Bacillus* sp., and cytochrome c_{551} (*29*). The K_m of reduced plumbagin is unaffected, and the turnover number is decreased by the presence of cytochrome *c* with a calculated K_i of 5.2 μM, a value similar to its K_m. The rate of NO reduction in the presence of both cytochrome c_{551} and plumbagin is higher than the activity with cytochrome c_{551} alone, indicating simultaneous electron delivery from both plumbagin and cytochrome c_{551}.

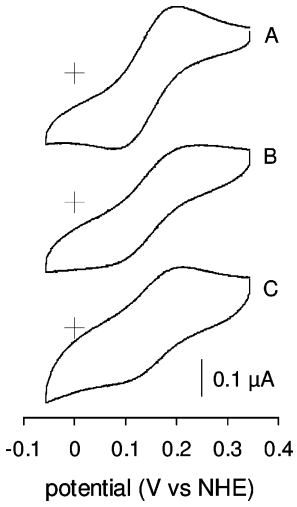

FIGURE 5: Cyclic voltammograms of cytochrome c_{551} (A), c_{550} (B), and c_{552} (C). The cytochromes were dissolved in 20 mM potassium phosphate buffer (pH 7.0, 1 mM EDTA and 0.03% lauryl maltoside). Protein concentrations were between 50 and 150 μM. The crosses indicate zero current. The scan rate was 2 mV/s (staircase parameters, $\alpha = 0.5$, $\Delta E = 1.22$ mV), with a filter constant of 1 s.

NO Tolerance in Vivo. To test whether the two NO reduction pathways in qCu$_A$NOR could play a potential role in NO detoxification, *in vivo* NO tolerance was determined in *B. azotoformans* and the denitrifyer *Pa. denitrificans* (Table 2). The results show that *B. azotoformans* is much more tolerant to high levels of NO than *Pa. denitrificans*. Further, the tolerance for NO of *B. azotoformans* grown under denitrifying conditions is much higher than in aerobically grown cells. The qCu$_A$NOR activity is expressed at much higher levels in denitrifying cells from *B. azotoformans* (0.64 μmol mg^{-1} min^{-1}) than in aerobically grown cells (0.022 μmol mg^{-1} min^{-1}). The same holds for *Pa. denitrificans*, which has cNOR activity much higher in denitrifying cells (0.56 μmol mg^{-1} min^{-1}) than in aerobic cells (0.009 μmol mg^{-1} min^{-1}).

DISCUSSION

The existence of a Cu$_A$ center in the menaquinol-dependent qCu$_A$NOR purified from *B. azotoformans* led to the question

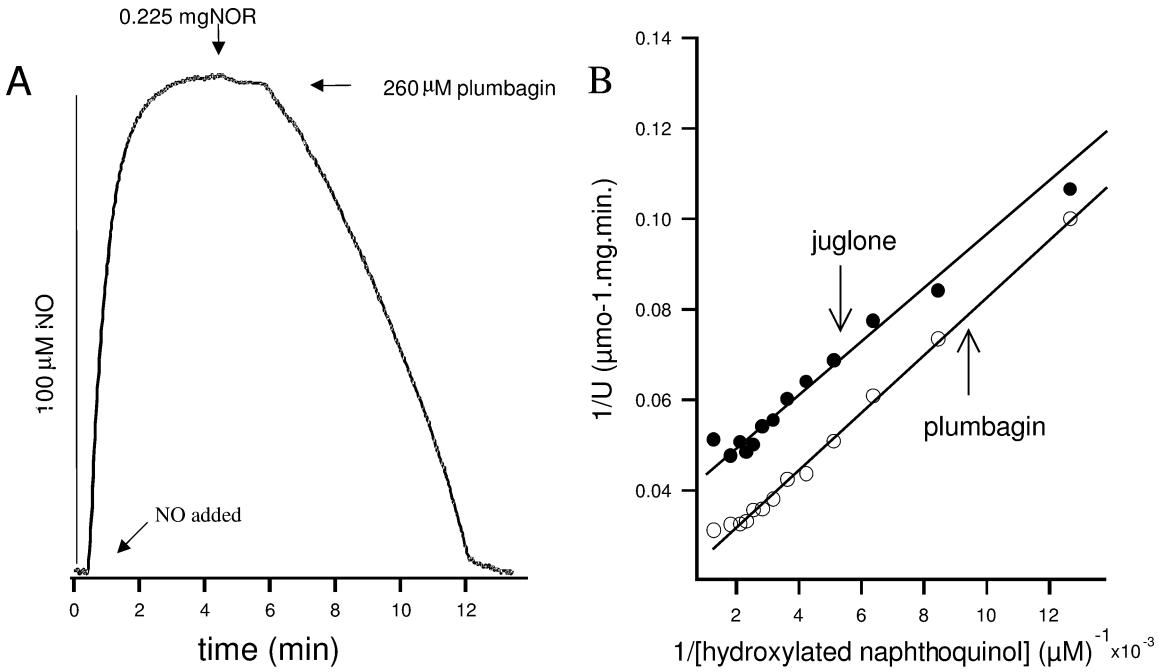

FIGURE 6: qCu_ANOR activity with hydroxylated naphthoquinols as electron donors. (A) Trace of qCu_ANOR activity using reduced plumbagin as the electron donor. (B) Data points of qCu_ANOR activity were measured using juglone as the electron donor (●) and plumbagin (○). The lines through the data points are linear least-squares fits (—).

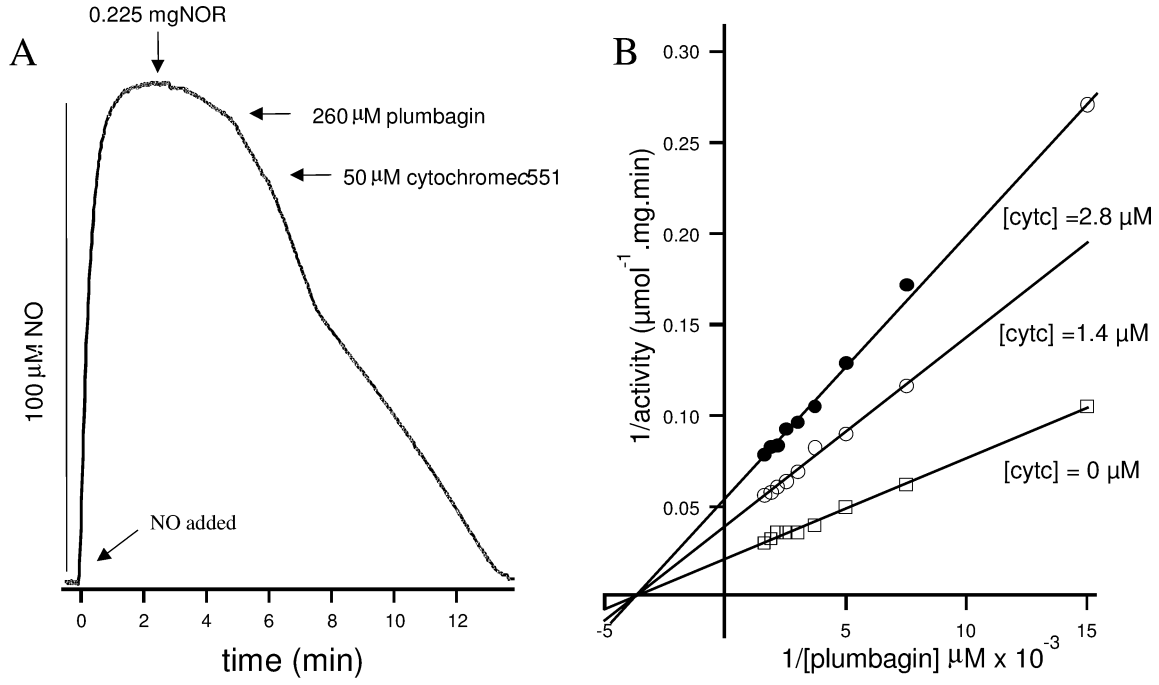

FIGURE 7: Inhibition of menaquinol-dependent activity by membrane-bound cytochrome c_{551}. (A) qCu_ANOR was added to the buffer containing 10 mM ascorbic acid to regenerate reduced cytochrome c_{551}; after ~2 min, reduced plumbagin was added. Approximately 1 min later, cytochrome c_{551} was added (B). Various concentrations of cytochrome c_{551} and plumbagin were used as electron donors for qCu_A-NOR, yielding a pattern typical for a noncompetitive inhibition.

of whether an endogenous cytochrome *c* might serve as a physiological electron donor to this enzyme. The results in this paper support this suggestion.

We have successfully purified three negatively charged *c* cytochromes from the *B. azotoformans* membranes. The molecular masses of these *c* cytochromes are ~11.0 kDa. The midpoint potentials of the membrane-bound *c* cytochromes are approximately 100 mV lower than that of horse heart cytochrome *c*. The peak separation observed in the cyclic voltammetry experiments is larger than the value of 58 mV expected for diffusion-limited voltammetry, indicative of slow electron exchange between the heme prosthetic group and the electrode surface. The heterogeneous electron transfer rate constants (at $E = E_m$) are estimated to be $\sim 6 \times 10^{-4}$, 3×10^{-4}, and 5×10^{-4} cm/s for cytochrome c_{551}, c_{550}, and c_{552}, respectively (*30*). Because a freshly polished glassy carbon surface is slightly hydrophobic and also contains negatively charged carboxyl groups, we speculate that the preferred orientation of the cytochromes is with the hydrophobic tail toward the electrode, while the heme is most

Table 2: Percentage of Cells Surviving 5% NO Treatment[a]

	% surviving cells	
	aerobically grown	anaerobically grown on NO_3^-
B. azotoformans	9.6	92.1
Pa. denitrificans	0.0	0.6

[a] Cells from aerobically or anaerobically (NO_3^-) grown cultures of *B. azotoformans* and *Pa. denitrificans* were incubated for 2 h under an atmosphere of 5% NO, yielding 100 μM NO in solution. After this treatment, the cells were plated aerobically and the number of survivors was compared to the number for similarly treated control cells, incubated in the absence of NO. The number of plated control cells in each experiment was approximately 1.5×10^7.

likely located on the opposite, negatively charged side of the protein. Such an orientation results in a relatively large distance between the heme and the electrode surface and thus in slow electron transfer. Some effect on electron transfer kinetics due to binding of dodecyl maltoside to hydrophobic regions of either the protein or the electrode surface cannot be excluded. However, the polished glassy carbon is rich in oxidized carbon functionalities, and therefore most likely not sufficiently hydrophobic to promote the adsorption of a blocking monolayer of surfactant, especially not at the low concentration of dodecyl maltoside present in the solution (0.03%).

The low midpoint potentials of the three *B. azotoformans* cytochromes compared to that of mitochondrial cytochrome *c* are probably caused by their net negative charge, which stabilizes the ferric state, while the positive charge of the mitochondrial cytochromes favors the ferrous state. Only cytochrome c_{551}, which has a pI of 5.0 ± 0.5 and an E_m of 143 mV, was found to act as an electron donor to qCu_ANOR. The fact that the endogenous cytochrome c_{551} is a negatively charged cytochrome *c* with a midpoint potential lower than that of horse heart cytochrome *c* serves as an explanation why the highly positively charged horse heart cytochrome *c* with a 100 mV higher reduction potential cannot act as an electron donor to qCu_ANOR.

Unlike Gram-negative bacteria, Gram-positive bacteria lack an outer membrane and only have a small periplasmic space. Respiratory enzymes and electron carriers, which are normally located in the periplasmic space of Gram-negative bacteria, are usually membrane-bound in Gram-positive bacteria facing the periplasmic space (*31*−*36*). When purified cytochrome c_{551} was incubated with lipase, its mobility on butyl-Sepharose increased, yielding two new peaks indicating the presence of a covalently bound lipid consisting of two lipoyl moieties. The covalent attachment of lipids to protein N-terminal cysteine residues is an important general mechanism for anchoring small *c*-type cytochromes to the cytoplasmic membrane of Gram-positive bacteria (*23*) and also in Gram-negative bacteria such as the photosynthetic reaction center in *Rhodopseudomonas viridis* (*26*).

The ability of qCu_ANOR to accept electrons simultaneously via two different sites from endogenous cytochrome c_{551} and menaquinol is a unique feature among the nitric oxide reductases. In addition, such a dual electron pathway has up to now not been reported for any member of the superfamily of heme-copper oxidases. We suggest that the menaquinol binding site is located in subunit I close to the low-spin heme *b*, similar to the location of the quinol-binding site of cytochrome bo_3 oxidase from *Escherichia coli* (*37*). N-Terminal sequence analysis of subunit I of qCu_ANOR (residues 1−29, MTKKNTQEVVKEGREGIGTFIGVGIVGAV) indeed shows a considerable homology (21% identical and 52% similar) with cytochrome bo_3 oxidase from *E. coli*.

The unique electron transfer to qCu_ANOR led to the following question. Why does *B. azotoformans* need to employ both menaquinol and cytochrome c_{551} as electron donors for qCu_ANOR? It is generally observed that exogenous NO is toxic. Mammalian cells, including human cells,

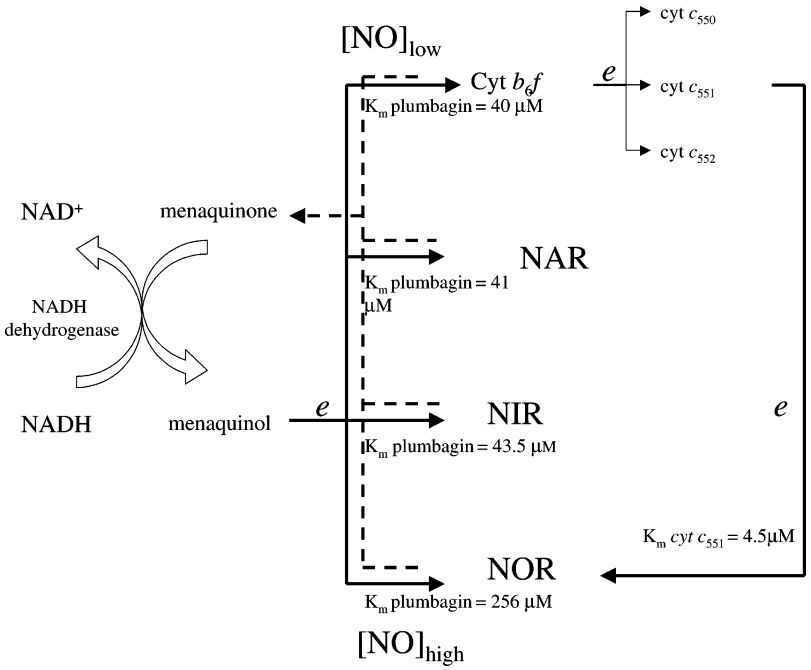

FIGURE 8: Electron flow diagram from NADH to NAR, NIR, and NOR. Two electron pathways from menaquinol to qCuANOR might exist postulated to be controlled by the NO concentration. Those are a direct electron transfer from menaquinol to qCu_ANOR (when the NO concentration is relatively high) and an extended electron pathway via b_6f complex, yielding a proton gradient and reduced cytochrome c_{551} (when the NO concentration is relatively low).

produce nitric oxide as an antimicrobial agent against a broad spectrum of pathogens such as *Neisseria meningitides* (*38*), *Citrobacter rodentium* (*39*), *Salmonella typhimurium* (*40*), and *Mycobacterium tuberculosis* (*41*). It is unclear, however, which NO concentration is lethal. A knockout mutation of NO reductase in *Ps. stutzeri* shows a denitrification-negative phenotype due to accumulation of NO in the growth medium (*42*). In the Gram-negative bacteria, such as *Ps. stutzeri* and *Ps. aeruginosa* and *Pa. denitrificans*, the concentration of NO during steady-state denitrification is less than 65 nM (*1*, *43*). It has been reported that *B. azotoformans* vigorously grows in the presence of nitrate, nitrite, and nitrous oxide (*44*). Under 10% NO (200 μM in solution), the cell suspension was reported to reduce NO, although growth was absent (*44*). We observed that anaerobically induced *B. azotoformans* survived after incubation for 2 h under 5% NO (100 μM), in contrast to *Pa. denitrificans* (Table 2). It is further seen that aerobically grown *B. azotoformans* is much more NO tolerant than anaerobically grown *Pa. denitrificans*, even though in both organisms the activities of their respective NO reductases are low. However, the finding that anaerobically grown cells of *B. azotoformans* but not *Pa. denitrificans* are much more NO tolerant than aerobically grown cells, in conjunction with their greatly increased levels of qCu_ANOR, strongly suggests that this enzyme is specifically responsible for the increased NO tolerance in addition to its role in denitrification.

The fact that anaerobically grown *Pa. denitrificans* which has similar levels of NO reductase activity is not NO tolerant further indicates that it might be the bifunctional activity of the qCu_ANOR, especially the menaquinol-dependent one, which is responsible for this. In this respect, the observation that pathogens employ qNORs rather than cNORs may be relevant. We propose that at high NO concentrations a fast electron delivery to qCu_ANOR might be needed for NO detoxification. This is effectuated by menaquinol directly, thus bypassing the b_6f complex. However, when the NO concentration reaches the steady-state value for dissimilatory denitrification, more menaquinol will be oxidized via the b_6f complex pathway, yielding reduced *c* cytochromes, including cytochrome c_{551}, which subsequently inhibits the menaquinol-dependent qCu_ANOR activity (Figure 8). This proposal is supported by two experimental observations. First, the direct electron pathway from menaquinol analogue plumbagin has a 4-fold greater maximal activity than the pathway via cytochrome c_{551}. The second is the relative K_m values for plumbagin for the various enzymes. We found a K_m value for plumbagin of 40 μM when it couples to cytochrome *c* reduction via the b_6f complex, and of 41 and 43.5 μM for nitrate reductase and nitrite reductase, respectively. These latter values are all much lower than the K_m for plumbagin for the reduction of NO by qCu_ANOR (256 μM). Unlike cytochrome *c* oxidase, the reduction of NO by NOR is not coupled to proton translocation (*45*−*47*). Therefore, the cell does not energetically benefit from the menaquinol-dependent qCu_ANOR activity. This is consistent with the finding that even though *B. azotoformans* survives high NO concentrations (Table 2), the cells did not markedly grow. We propose that the menaquinol pathway, which has a 4-fold greater maximal activity than the pathway via cytochrome c_{551}, and which is absent, for example, from *Pa. denitrificans*, is used for NO detoxification, whereas electron donation via the endogenous *c* cytochrome involves the cytochrome b_6f complex and serves the bioenergetic needs of *B. azotoformans*.

REFERENCES

1. Zumft, W. G. (1997) Cell biology and molecular basis of denitrification, *Microbiol. Mol. Biol. Rev. 61*, 533−616.
2. Wasser, I. M., de Vries, S., Moënne-Loccoz, P., Schröder, I., and Karlin, K. D. (2002) Nitric oxide in biological denitrification: Fe/Cu metalloenzyme and metal complex NO(x) redox chemistry, *Chem. Rev. 102*, 1201−1234.
3. de Vries, D., and Schröder, I. (2002) Comparison between the nitric oxide reductase family and its aerobic relatives, the cytochrome oxidases, *Biochem. Soc. Trans. 30*, 662−667.
4. Kastrau, D. H., Heiss, B., Kroneck, P. M., and Zumft, W. G. (1994) Nitric oxide reductase from *Pseudomonas stutzeri*, a novel cytochrome *bc* complex. Phospholipid requirement, electron paramagnetic resonance and redox properties, *Eur. J. Biochem. 222*, 293−303.
5. Carr, G. J., and Ferguson, S. J. (1990) The nitric oxide reductase of *Paracoccus denitrificans*, *Biochem. J. 269*, 423−429.
6. Fujiwara, T., and Fukumori, Y. (1996) Cytochrome *cb*-type nitric oxide reductase with cytochrome *c* oxidase activity from *Paracoccus denitrificans* ATCC 35512, *J. Bacteriol. 178*, 1866−1871.
7. Girsch, P., and de Vries, S. (1997) Purification and initial kinetic and spectroscopic characterization of NO reductase from *Paracoccus denitrificans*, *Biochim. Biophys. Acta 1318*, 202−216.
8. Moir, J. W. B., and Ferguson, S. J. (1994) Properties of a *Paracoccus denitrificans* mutant deleted in cytochrome c_{550} indicate that a copper protein can substitute for this cytochrome in electron transport to nitrite, nitric oxide and nitrous oxide, *Microbiology 140*, 389−397.
9. Berks, B. C., Ferguson, S. J., Moir, J. W., and Richardson, D. J. (1995) Enzymes and associated electron transport systems that catalyse the respiratory reduction of nitrogen oxides and oxyanions, *Biochim. Biophys. Acta 1232*, 97−173.
10. Richardson, D. J., and Watmough, N. J. (1999) Inorganic nitrogen metabolism in bacteria, *Curr. Opin. Chem. Biol. 3*, 207−219.
11. Richardson, D. J. (2000) Bacterial respiration: a flexible process for a changing environment, *Microbiology 146* (Part 3), 551−571.
12. Cramm, R., Siddiqui, R. A., and Friedrich, B. (1997) Two isofunctional nitric oxide reductases in *Alcaligenes eutrophus* H16, *J. Bacteriol. 179*, 6769−6777.
13. De Vries, S., Strampraad, M. J. F., Lu, S., Moënne-Loccoz, P. and Schröder, I. (2003) Purification and characterization of the MQH_2: NO oxidoreductase (qNOR) from the hyperthermophilic Archaeon *Pyrobaculum aerophilum*, *J. Biol. Chem. 278*, 35861−35868.
14. Cramm, R., Pohlmann, A., and Friedrich, B. (1999) Purification and characterization of the single-component nitric oxide reductase from *Ralstonia eutropha* H16, *FEBS Lett. 460*, 6−10.
15. Suharti, Strampraad, M. J., Schröder, I., and de Vries, S. (2001) A novel copper A containing menaquinol NO reductase from *Bacillus azotoformans*, *Biochemistry 40*, 2632−2639.
16. Zimmermann, B. H., Nitsche, C. I., Fee, J. A., Rusnak, F., and Munck, E. (1988) Properties of a copper-containing cytochrome ba_3: a second terminal oxidase from the extreme thermophile *Thermus thermophilus*, *Proc. Natl. Acad. Sci. U.S.A. 85*, 5779−5783.
17. Wikstrom, M. (1989) Identification of the electron transfers in cytochrome oxidase that are coupled to proton-pumping, *Nature 338*, 776−778.
18. Malatesta, F., Nicoletti, F., Zickermann, V., Ludwig, B., and Brunori, M. (1998) Electron entry in a Cu_A mutant of cytochrome *c* oxidase from *Paracoccus denitrificans*. Conclusive evidence on the initial electron entry metal center, *FEBS Lett. 434*, 322−324.
19. Berks, B. C., Baratta, D., Richardson, J., and Ferguson, S. J. (1993) Purification and characterization of a nitrous oxide reductase from *Thiosphaera pantotropha*. Implications for the mechanism of aerobic nitrous oxide reduction, *Eur. J. Biochem. 212*, 467−476.
20. Richardson, D. J., Bell, L. C., McEwan, A. G., Jackson, J. B., and Ferguson, S. J. (1991) Cytochrome c_2 is essential for electron transfer to nitrous oxide reductase from physiological substrates in *Rhodobacter capsulatus* and can act as an electron donor to the reductase in vitro. Correlation with photoinhibition studies, *Eur. J. Biochem. 199*, 677−683.

21. Hagen, W. R. (1989) Direct electron transfer of redox proteins at the bare glassy carbon electrode, *Eur. J. Biochem. 182*, 523−530.
22. Thomas, P. E., Ryan, D., and Levin, W. (1976) An improved staining procedure for the detection of the peroxidase activity of cytochrome P450 on sodium dodecyl sulfate polyacrylamide gels, *Anal. Biochem. 75*, 168−176.
23. Noguchi, S., Yamazaki, T., Yaginuma, A., Sakamoto, J., and Sone, N. (1994) Overexpression of membrane-bound cytochrome *c*-551 from thermophilic *Bacillus* PS3 in *Bacillus stearothermophilu*s K1041, *Biochim. Biophys. Acta 1188*, 302−310.
24. David, P. S., Dutt, P. S., Wathen, B., Jia, Z., and Hill, B. C. (2000) Characterization of a structural model of membrane bound cytochrome *c*-550 from *Bacillus subtilis*, *Arch. Biochem. Biophys. 377*, 22−30.
25. von Wachenfeldt, C., and Hederstedt, L. (1993) Physico-chemical characterisation of membrane-bound and water-soluble forms of *Bacillus subtilis* cytochrome *c*-550, *Eur. J. Biochem. 212*, 499−509.
26. Hucke, O., Schiltz, E., Drews, G., and Labahn, A. (2003) Sequence analysis reveals new membrane anchor of reaction centre-bound cytochromes possibly related to PufX, *FEBS Lett. 535*, 166−170.
27. Fujiwara, Y., Oka, M., Hamamoto, T., and Sone, N. (1993) Cytochrome *c*-551 of the thermophilic bacterium PS3, DNA sequence and analysis of the mature cytochrome, *Biochim. Biophys. Acta 1144*, 213−219.
28. Rothery, R. A., Chatterjee, I., Kiema, G., McDermott, M. T., and Weiner, J. H. (1998) Hydroxylated naphthoquinones as substrates for *Escherichia coli* anaerobic reductases, *Biochem. J. 332* (Part 1), 35−41.
29. Fersht, A. (1999) *Structure and mechanism in protein science. A guide to enzyme catalysis and protein folding*, W. H. Freeman and Co., New York.
30. Bard, A. J., and Faulkner, L. R. (2001) *Electrochemical methods: fundamentals and applications*, 2nd ed., Wiley, New York.
31. Hole, U. H., Vollack, K. U., Zumft, W. G., Eisenmann, E., Siddiqui, R. A., Friedrich, B., and Kroneck, P. M. (1996) Characterization of the membranous denitrification enzymes nitrite reductase (cytochrome cd1) and copper-containing nitrous oxide reductase from *Thiobacillus denitrificans*, *Arch. Microbiol. 165*, 55−61.
32. Sakamoto, J., Handa, Y., and Sone, N. (1997) A novel cytochrome $b(o/a)_3$-type oxidase from *Bacillus stearothermophilu*s catalyzes cytochrome *c*-551 oxidation, *J. Biochem. 122*, 764−771.
33. Nielsen, J. B., and Lampen, J. O. (1982) Membrane-bound penicillinases in Gram-positive bacteria, *J. Biol. Chem. 257*, 4490−4495.
34. Nielsen, J. B., and Lampen, J. O. (1982) Glyceride-cysteine lipoproteins and secretion by Gram-positive bacteria, *J. Bacteriol. 152*, 315−322.
35. Gilson, E., Alloing, G., Schmidt, T., Claverys, J. P., Dudler, R., and Hofnung, M. (1988) Evidence for high affinity binding-protein dependent transport systems in gram-positive bacteria and in Mycoplasma, *EMBO J. 7*, 3971−3974.
36. Navarre, W. W., and Schneewind, O. (1999) Surface proteins of gram-positive bacteria and mechanisms of their targeting to the cell wall envelope, *Microbiol. Mol. Biol. Rev. 63*, 174−229.
37. Abramson, J., Larsson, G., Byrne, B., Puustinen, A., Garcia-Horsman, A., and Iwata, S. (2000) Purification, crystallization and preliminary crystallographic studies of an integral membrane protein, cytochrome bo_3 ubiquinol oxidase from *Escherichia coli*, *Acta Crystallogr. D56* (Part 8), 1076−1078.
38. De Groote, M. A., and Fang, F. C. (1995) NO inhibitions: antimicrobial properties of nitric oxide, *Clin. Infect. Dis. 21* (Suppl. 2), S162−S165.
39. Vallance, B. A., Deng, W., De Grado, M., Chan, C., Jacobson, K., and Finlay, B. B. (2002) Modulation of inducible nitric oxide synthase expression by the attaching and effacing bacterial pathogen *Citrobacter rodentium* in infected mice, *Infect. Immun. 70*, 6424−6435.
40. Alam, M. S., Akaike, T., Okamoto, S., Kubota, T., Yoshitake, J., Sawa, T., Miyamoto, Y., Tamura, F., and Maeda, H. (2002) Role of nitric oxide in host defense in murine salmonellosis as a function of its antibacterial and antiapoptotic activities, *Infect. Immun. 70*, 3130−3142.
41. Ehrt, S., Schnappinger, D., Bekiranov, S., Drenkow, J., Shi, S., Gingeras, T. R., Gaasterland, T., Schoolnik, G., and Nathan, C. (2001) Reprogramming of the macrophage transcriptome in response to interferon-γ and *Mycobacterium tuberculosis*: signaling roles of nitric oxide synthase-2 and phagocyte oxidase, *J. Exp. Med. 194*, 1123−1140.
42. Braun, C., and Zumft, W. G. (1991) Marker exchange of the structural genes for nitric oxide reductase blocks the denitrification pathway of *Pseudomonas stutzeri* at nitric oxide, *J. Biol. Chem. 266*, 22785−22788.
43. Goretski, J., Zafiriou, O. C., and Hollocher, T. C. (1990) Steady-state nitric oxide concentrations during denitrification, *J. Biol. Chem. 265*, 11535−11538.
44. Pichinoty, F., Durand, M., Job, C., Mandel, M., and Garcia, J. L. (1978) Morphological, physiological and taxonomic studies of *Bacillus azotoformans*, *Can. J. Microbiol. 24*, 608−617.
45. Carr, G. J., Page, M. D., and Ferguson, S. J. (1989) The energy-conserving nitric-oxide-reductase system in *Paracoccus denitrificans*. Distinction from the nitrite reductase that catalyses synthesis of nitric oxide and evidence from trapping experiments for nitric oxide as a free intermediate during denitrification, *Eur. J. Biochem. 179*, 683−692.
46. Bell, L. C., Richardson, D. J., and Ferguson, S. J. (1992) Identification of nitric oxide reductase activity in *Rhodobacter capsulatus*: the electron transport pathway can either use or bypass both cytochrome c_2 and the cytochrome bc_1 complex, *J. Gen. Microbiol. 138* (Part 3), 437−443.
47. Hendriks, J. H., Jasaitis, A., Saraste, M., and Verkhovsky, M. I. (2002) Proton and electron pathways in the bacterial nitric oxide reductase, *Biochemistry 41*, 2331−2340.

BI0488101